LETTER

doi:10.1038/nature09727

CREBBP mutations in relapsed acute lymphoblastic leukaemia

Charles G. Mullighan[1]*, Jinghui Zhang[2]*, Lawryn H. Kasper[3], Stephanie Lerach[3], Debbie Payne-Turner[1], Letha A. Phillips[1], Sue L. Heatley[1], Linda Holmfeldt[1], J. Racquel Collins-Underwood[1], Jing Ma[4], Kenneth H. Buetow[5,6], Ching-Hon Pui[7], Sharyn D. Baker[8], Paul K. Brindle[3] & James R. Downing[1]

Relapsed acute lymphoblastic leukaemia (ALL) is a leading cause of death due to disease in young people, but the biological determinants of treatment failure remain poorly understood. Recent genome-wide profiling of structural DNA alterations in ALL have identified multiple submicroscopic somatic mutations targeting key cellular pathways[1,2], and have demonstrated substantial evolution in genetic alterations from diagnosis to relapse[3]. However, DNA sequence mutations in ALL have not been analysed in detail. To identify novel mutations in relapsed ALL, we resequenced 300 genes in matched diagnosis and relapse samples from 23 patients with ALL. This identified 52 somatic non-synonymous mutations in 32 genes, many of which were novel, including the transcriptional coactivators *CREBBP* and *NCOR1*, the transcription factors *ERG*, *SPI1*, *TCF4* and *TCF7L2*, components of the Ras signalling pathway, histone genes, genes involved in histone modification (*CREBBP* and *CTCF*), and genes previously shown[1,2] to be targets of recurring DNA copy number alteration in ALL. Analysis of an extended cohort of 71 diagnosis–relapse cases and 270 acute leukaemia cases that did not relapse found that 18.3% of relapse cases had sequence or deletion mutations of *CREBBP*, which encodes the transcriptional coactivator and histone acetyltransferase CREB-binding protein (CREBBP, also known as CBP)[4]. The mutations were either present at diagnosis or acquired at relapse, and resulted in truncated alleles or deleterious substitutions in conserved residues of the histone acetyltransferase domain. Functionally, the mutations impaired histone acetylation and transcriptional regulation of CREBBP targets, including glucocorticoid responsive genes. Several mutations acquired at relapse were detected in subclones at diagnosis, suggesting that the mutations may confer resistance to therapy. These results extend the landscape of genetic alterations in leukaemia, and identify mutations targeting transcriptional and epigenetic regulation as a mechanism of resistance in ALL.

Acute lymphoblastic leukaemia (ALL) is the commonest childhood malignancy[5], and is a leading cause of cancer-related death in young people. Several structural chromosomal alterations in ALL, including rearrangement of *MLL* and the Philadelphia chromosome[6] are associated with a high risk of treatment failure and relapse. However, many ALL cases that fail therapy lack these alterations, and the biological basis of treatment failure in these cases is poorly understood. Genome-wide profiling of ALL has identified multiple recurring submicroscopic genetic alterations targeting lymphoid development, cell cycle regulation, tumour suppression and apoptosis[1,2], and has identified genetic alterations that predict a high risk of relapse, including deletion of *IKZF1* (encoding the transcription factor IKAROS)[7,8]. Moreover, profiling of structural DNA alterations in matched diagnosis and relapse samples has demonstrated that in the majority of cases there are substantial differences in the complement of genetic lesions between diagnosis and relapse, although the predominant clones at both stages of disease share a common ancestral origin[3,9]. The predominant clones at relapse are commonly present at low levels at diagnosis, suggesting that specific genetic alterations may confer resistance to therapy. Frequently acquired lesions at relapse include deletions of *CDKN2A/B*, *ETV6* and *IKZF1*[3,9]. However, a detailed analysis of sequence variation in ALL has not been performed.

To identify novel sequence mutations in relapsed ALL, we resequenced 300 genes in matched diagnosis–relapse samples from 23 children with B-cell progenitor ALL. Cases studied included B-cell progenitor ALL with high hyperdiploidy ($N = 3$), *TCF3-PBX1* ($N = 1$), *ETV6-RUNX1* ($N = 3$), rearrangement of *MLL* ($N = 3$), *BCR-ABL1* ($N = 3$), and low hyperdiploid, pseudodiploid, or miscellaneous karyotypes ($N = 10$) (Supplementary Table 1). We sequenced genes known to be mutated in leukaemia and cancer, and those that encode pathway components targeted by recurring copy number alteration in ALL, tumour suppressors, cell cycle regulators, tyrosine kinases, and genes encoding DNA repair proteins (Supplementary Table 2). We identified 52 somatic (non-inherited) protein coding variants in 32 genes in 20 cases (mean 2.5 variants per case, range 0–5) (Supplementary Table 3). Somatic mutations were identified in genes previously known to be mutated in haematopoietic malignancies and ALL, including the ETS-family transcription factor gene *ETV6* ($N = 1$); the Janus kinase gene *JAK1* ($N = 1$); the Ras pathway genes *NRAS* ($N = 5$; Supplementary Table 4 and Supplementary Fig. 1), *KRAS* ($N = 2$), *NF1* ($N = 3$) and *PTPN11* ($N = 2$); the B-lymphoid transcription factor gene *PAX5* ($N = 2$); the U3 ubiquitin ligase gene *FBXW7* ($N = 1$); the histone methyltransferase gene *EZH2* ($N = 1$); and the tumour suppressor gene *TP53* ($N = 2$). In addition, we observed patterns of evolution of sequence variations between diagnosis and relapse that recapitulated those observed for DNA copy number alterations in ALL[3] (Table 1, Supplementary Results and Supplementary Table 4).

A novel finding was somatic coding mutations in *CREBBP* (or *CBP*, encoding CREB-binding protein) in four of 23 cases sequenced (Supplementary Table 5). *CREBBP* was selected for sequencing by identifying recurring focal deletions involving the gene. CREBBP and its paralogue, EP300 (p300) are transcriptional coactivators with multiple functions in development and haematopoiesis[4,10,11]. Both are molecular scaffolds that interact with a diverse range of transcription factors, regulate transcription by acetylation of histone and non-histone targets, and may regulate protein turnover by E4 polyubiquitin ligase activity. *CREBBP* and *EP300* are known targets of translocations in acute leukaemia (for example, *MLL-EP300*, *MLL-CREBBP*, *MOZ-CREBBP* and *MOZ-EP300*)[12]. Inherited *CREBBP* mutations and

[1]Department of Pathology, St Jude Children's Research Hospital, Memphis, Tennessee 38105, USA. [2]Department of Computational Biology, St Jude Children's Research Hospital, Memphis, Tennessee 38105, USA. [3]Department of Biochemistry, St Jude Children's Research Hospital, Memphis, Tennessee 38105, USA. [4]The Hartwell Center for Bioinformatics and Biotechnology, St Jude Children's Research Hospital, Memphis, Tennessee 38105, USA. [5]National Cancer Institute Center for Bioinformatics, National Cancer Institute, Rockville, Maryland 20892, USA. [6]Laboratory of Population Genetics, National Cancer Institute, National Institutes of Health, Bethesda, Maryland 20892, USA. [7]Department of Oncology, St Jude Children's Research Hospital, Memphis, Tennessee 38105, USA. [8]Department of Pharmaceutical Sciences, St Jude Children's Research Hospital, Memphis, Tennessee 38105, USA.
*These authors contributed equally to this work.

Table 1 | Recurrent mutations in 23 matched diagnosis–relapse ALL cases

Gene	*N*	Present at diagnosis and relapse	Present at diagnosis only	Present at relapse only	Description/function
ASMTL	3	2		1	Acetylserotonin O-methyltransferase-like
CREBBP	4	3		1	Transcriptional coactivator, histone and non-histone acetyl transferase, ubiquitin ligase
ERG	2			2	ETS family transcription factor
FLT3	2		1	1	Receptor tyrosine kinase, Ras pathway
KRAS	3	2		1	Ras pathway
NF1	2		2		Ras pathway
NRAS	5	2	2	1	Ras pathway
PAX5	2	1	1		B cell development
PTPN11	2	1		1	Ras pathway
TP53	2			2	Tumour suppressor
TUSC3	2	2			Tumour suppressor candidate

deletions result in the Rubinstein–Taybi syndrome, a developmental disorder characterized by dysmorphology, intellectual impairment, and an increased susceptibility to solid tumours[13,14]. Homozygous deletion of *Crebbp* or *Ep300* is lethal in mice owing to developmental abnormalities, and *Crebbp*$^{+/-}$ mice show defects in B lymphoid development, and an increased incidence of haematopoietic tumours[15]. Although *CREBBP* and *EP300* sequence mutations have been reported in solid tumours[16,17] and rare *EP300* mutations have been detected in an ALL cell line and myelodysplasia[18], there are no prior reports of *CREBBP* sequence mutations in haematologic malignancies.

To define the frequency of *CREBBP* and *EP300* mutations in acute leukaemia, we sequenced these genes in an additional 318 cases of paediatric leukaemia. These additional cases included matched diagnosis and relapse samples from 48 children with ALL, and diagnosis samples from children with ALL ($N = 170$) and acute myeloid leukaemia (AML, $N = 100$)[19] that did not relapse. Single nucleotide polymorphism (SNP) microarray DNA copy number alteration and loss-of-heterozygosity data were available for all cases sequenced[1,20,21]. We also examined DNA copy number alterations in a further 107 ALL cases that were not sequenced[1,3,20]. In addition, *CREBBP* was sequenced in 58 ALL and AML cell lines. Remarkably, 13 of 71 (18.3%) of relapsed ALL cases harboured either tumour-acquired (non-inherited) sequence alterations ($N = 13$) or focal deletions ($N = 2$) of *CREBBP* (Supplementary Table 5 and Supplementary Fig. 2). In contrast, *CREBBP* alterations in cases of childhood acute leukaemia that did not relapse were rare, with only one additional *CREBBP* mutation identified in 200 AML and ALL cases sequenced (ALL patient Hyperdiploid-#22, C1408Y, Supplementary Table 5). Furthermore, three of 307 ALL cases with SNP array data had focal *CREBBP* deletions at diagnosis (Supplementary Table 5 and Supplementary Fig. 2). *CREBBP* alterations were not observed in AML.

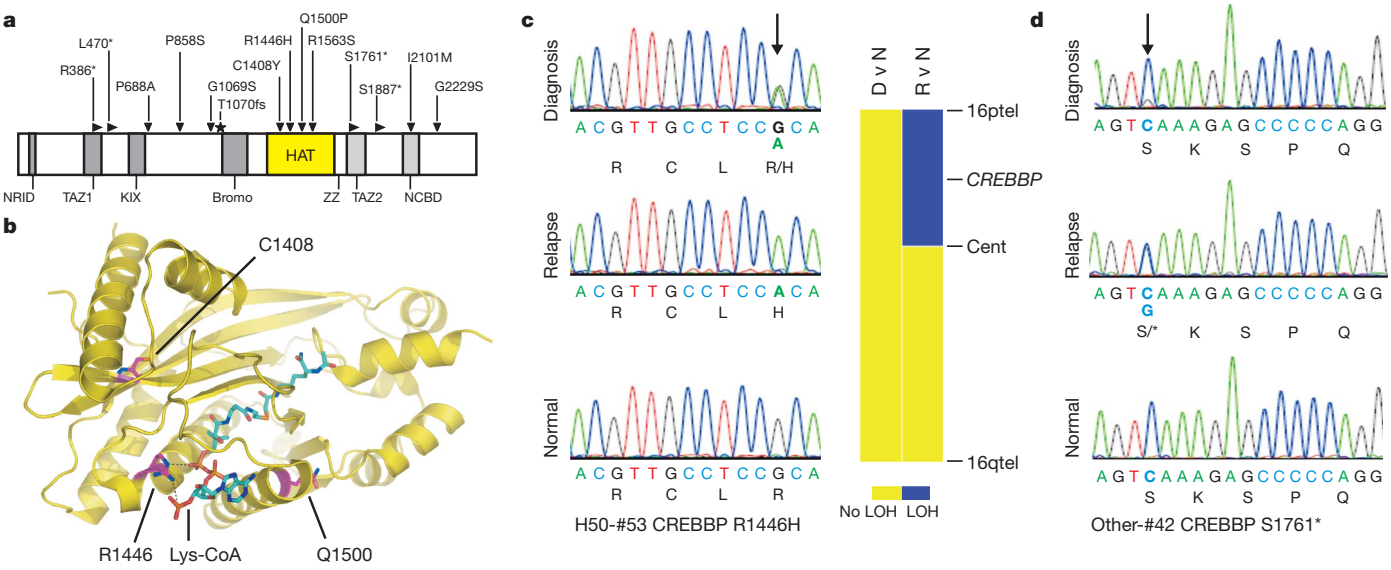

Figure 1 | *CREBBP* sequence mutations in relapsed ALL. **a**, Most variants are missense mutations in CREBBP domains involved in histone acetylation or transcription factor recruitment, or result in protein truncation. NRID, nuclear-receptor-interaction domain; TAZ1/2, transcriptional-adaptor zinc-finger 1/2; KIX, KID-binding domain; Bromo, bromodomain; HAT, histone acetyltransferase domain; ZZ, zinc-binding domain near the dystrophin WW domain; NCBD, nuclear-receptor coactivator-binding domain. **b**, The locations of CREBBP HAT mutations are shown using the crystal structure of the EP300 HAT domain complexed with its bisubstrate inhibitor, Lys-CoA (blue)[22]. CREBBP R1446 (equivalent to EP300 R1410) contacts phosphates of the CoA moiety of the inhibitor (salt bridges are shown as dashed lines), and the R1446H mutation is predicted to disrupt substrate binding. Q1500P (EP300 Q1464) is predicted to disrupt the α4 helix, which stabilizes the substrate binding loop L1 between the β5 strand and the α4 helix. C1408H (EP300 C1372) is predicted to disrupt the hydrophobic core that involves both the amino and carboxy termini of the HAT domain. R1563 cannot be shown because this residue lies in a proteolytically sensitive autoacetylation loop that was deleted in order to generate the crystal structure[22]. **c**, Sequence traces (labelled with nucleotide, and corresponding amino acid residues R, C, L and R/H) showing duplication of the R1446H mutation at relapse for patient H50-#53. This mutation was heterozygous at diagnosis and absent in the matched normal sample. There is copy-neutral loss of heterozygosity (LOH) of chromosome 16p at relapse but not at diagnosis. D v N is the LOH analysis of diagnosis sample compared to matched normal sample; R v N is the relapse compared to matched normal sample. Cent, centromere; 16ptel, chromosome 16p telomere; 16qtel, chromosome 16q telomere. **d**, Sequence traces (labelled with nucleotide, and corresponding amino acid residues S, K, P and Q). In patient Other-#42, CREBBP mutations are present in subclones at diagnosis, and emerge in the predominant clone at relapse. The S1761* mutation is heterozygous in the relapse sample, absent in the matched normal sample, and appears as a minor peak in the diagnosis sample. Presence of this mutation in a subpopulation of cells at diagnosis was confirmed by PCR, cloning and bidirectional sequencing of multiple colonies of the diagnosis sample (data not shown).

Only one *EP300* mutation was detected in the 71 cases that relapsed, a missense mutation (P925L) acquired at relapse. The identified *CREBBP* mutations resulted in amino acid substitutions, most commonly in the histone acetyltransferase (HAT) domain, or truncating frameshift or nonsense changes (Fig. 1a). The HAT mutations involved highly conserved residues (Supplementary Fig. 3). Modelling of the predicted effects of the CREBBP HAT mutations using the crystal structure of the highly homologous EP300 HAT domain[22] demonstrated that the mutations are likely to disrupt the structure of the domain or its interaction with substrates (Fig. 1b).

Notably, *CREBBP* mutations present at diagnosis were retained or duplicated at relapse. Three cases had biallelic *CREBBP* mutations, either compound heterozygosity for different mutations, or homozygosity for a single mutation (Q1500P). Q1500P, but none of the other mutations identified in ALL, is also observed in Rubinstein–Taybi syndrome[13]. Homozygosity for this mutation was accompanied by DNA copy-neutral loss-of-heterozygosity (acquired uniparental disomy) of chromosome 16p in both diagnosis and relapse samples, but not the germline sample in this case. This was identified on analysis of SNP microarray genotype data for this patient, indicating that one copy of 16p containing the wild-type *CREBBP* allele had been deleted, while the remaining copy of 16p harbouring the Q1500P allele had been duplicated. One case (patient Hyperdiploid-#53) had a heterozygous HAT domain mutation (R1446H) at diagnosis that was homozygous at relapse with accompanying copy-neutral loss-of-heterozygosity of 16p, again indicating duplication of the mutated allele in the predominant relapse clone (Fig. 1c). Furthermore, three mutations detected at relapse (T1070fs, S1761* and I2101M) were detected at low levels in the diagnosis sample (Fig. 1d).

Together, the high frequency of *CREBBP* mutations in relapsed ALL, the persistence, reduplication or emergence of mutations from diagnosis to relapse, and the location of the mutations in key CREBBP functional domains suggest that these alterations impair CREBBP function and influence treatment responsiveness. CREBBP is expressed in

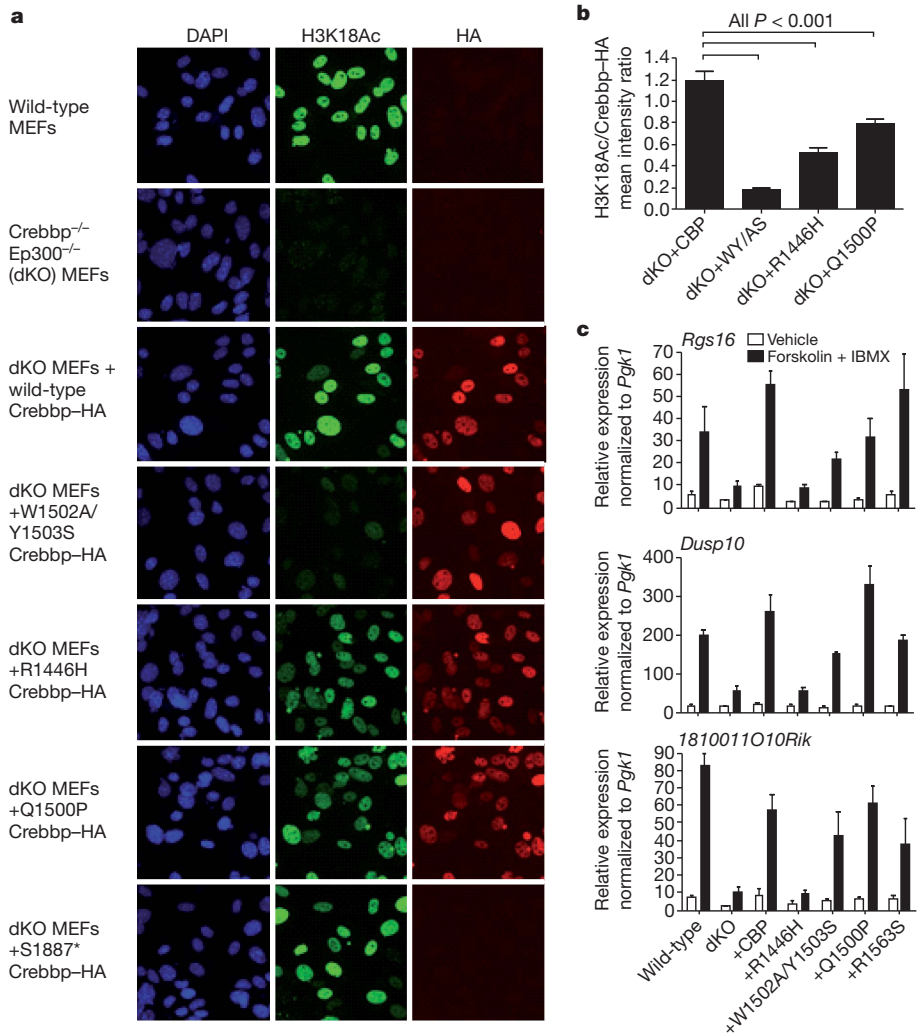

Figure 2 | CREBBP mutations impair histone acetylation and multiple gene expression programs. **a**, Immunofluorescence to detect histone H3 lysine 18 acetylation (H3K18Ac) in nontransduced wild-type MEFs, *Crebbp*$^{\Delta flox/\Delta flox}$;*Ep300*$^{\Delta flox/\Delta flox}$ (dKO) MEFs and dKO MEFs transduced with retrovirus expressing wild type (+Crebbp) and mutant haemagglutinin (HA)-tagged Crebbp. Four independent experiments with separate controls were performed, one of which is shown. S1887* truncates the protein before the C-terminal HA-tag, but is predicted to retain the HAT domain. **b**, Quantification of H3K18Ac mean signal intensity per nucleus relative to the HA-tagged Crebbp retrovirus mean signal intensity. Values are mean ± s.e.m.; 40–61 nuclei quantified per retrovirus. Only nuclei that have an HA-tag (Crebbp-HA) signal greater than 2.5-fold above background were included. Data are expressed as the ratio of the mean H3K18Ac signal intensity for each nucleus to the mean HA signal intensity for the same nuclei. The *P* value shown is from a Tukey post-test of one-way analysis of variance (ANOVA); mean ± standard error of the mean. **c**, Quantitative reverse transcription (RT)–PCR gene expression data from dKO MEFs transduced with wild-type or mutant CBP, and treated with ethanol (vehicle) or with 10 μM forskolin + 100 μM IBMX for 90 min. W1502A/Y1503S (WY/AS) is a previously described mutation that inactivates HAT enzymatic activity[30]. Gene expression was normalized to expression of *Pgk1*. $N = 3–7$.

leukaemic cells and normal B-cell progenitors (Supplementary Fig. 4), and the mutant *CREBBP* alleles are expressed in ALL cell lines harbouring mutations (Supplementary Table 6 and Supplementary Fig. 5).

We investigated the functional effect of the mutations in mice. We examined the histone acetylation and transcriptional activities of wild-type and mutant *Crebbp* alleles expressed in $Crebbp^{\Delta flox/\Delta flox}$;$Ep300^{\Delta flox/\Delta flox}$ (CBP/p300 Cre-deleted double knockout, or dKO) primary murine embryonic fibroblasts (MEFs)[23–25] (Fig. 2 and Supplementary Figs 6–10). The CREBBP HAT mutations resulted in diminished acetylation of histone H3 lysine 18 (H3K18), a known acetylation substrate of CREBBP[25] (Fig. 2a and b). Notably, the acetylation was attenuated but not blocked, and differed between HAT mutants (Fig. 2a and b). The Rubinstein–Taybi syndrome Q1500P mutation resulted in only a modest reduction in acetylation despite being predicted to disrupt a key α helix in the HAT domain (Fig. 1a). This suggests that HAT mutants have additional deleterious effects beyond impairing histone acetylation, that H3K18 is not the critical substrate, or that attenuated HAT activity is sufficient for the phenotype. To investigate these possibilities, we examined the effects of the CREBBP mutations on the expression of Crebbp target genes and cell proliferation in dKO MEFs transduced with retrovirus expressing wild-type and mutant Crebbp complementary DNAs (Fig. 2c and Supplementary Figs 6–10). We tested mutations in the HAT domain, as well as S1761*, S1887* and I2101M, which are predicted to affect the nuclear coactivator binding domain (Fig. 1a). Interestingly, the HAT mutants result in reduced expression of cyclic-AMP-responsive CREB target genes (Fig. 2c and Supplementary Figs 6–8). Furthermore, many of the mutants tested also impaired cell proliferation (Supplementary Fig. 11). Truncating mutations within the carboxy-terminal region of the HAT domain affected the expression of double-stranded RNA and glucocorticoid-receptor-responsive genes (Supplementary Fig. 8j–k and Supplementary Figs 9–10), consistent with the role of the nuclear coactivator binding domain in these pathways. The magnitude of reduced expression depended on the target gene, the specific mutation and the pathway, but the finding that CREBBP mutations result in impaired expression of glucocorticoid-receptor-responsive genes is particularly notable. The glucocorticoid dexamethasone is a mainstay of therapy for ALL, and poor responsiveness to steroid therapy is strongly associated with poor treatment outcome[26]. Accordingly, we examined responsiveness to dexamethasone and the class I/II HDAC inhibitor vorinostat in a panel of T-lineage ALL cell lines with wild-type or mutant *CREBBP* alleles. This demonstrated dexamethasone resistance in the majority of cell lines, but sensitivity to vorinostat at clinically useful concentrations (half-maximum inhibitory concentration IC_{50} below 1 μM) in the majority of cell lines tested (Supplementary Table 7 and Supplementary Fig. 12). This suggests that multiple mechanisms are likely to influence glucocorticoid responsiveness, but that HDAC inhibitor therapy may be useful in steroid-resistant ALL.

These findings show that detailed analysis of sequence alterations in relapsed ALL can identify novel genetic alterations that are likely to be involved in the pathogenesis of treatment failure. Approximately 10% of the genes sequenced harboured somatic sequence mutations with multiple mutations involving transcriptional regulators and coactivators, many of which are targeted by other structural genetic alterations in ALL, including deletions and translocations (for example, *PAX5, ERG, ETV6, CREBBP* and *EP300*). These results, together with those of Pasqualucci *et al.* identifying a high frequency of *CREBBP* and *EP300* mutations in diffuse large B-cell and follicular lymphoma[27], also identify *CREBBP* and *EP300* as new targets of recurring mutation in a range of lymphoid malignancies. The observation that the *CREBBP* mutations impair regulation of glucocorticoid-responsive genes, and that the mutations are selected for at relapse, suggests that these alterations may influence response to therapy and the likelihood of relapse. These results are also of clinical relevance, because they suggest that therapeutic approaches directed at modulating protein acetylation[28] may be useful in high-risk ALL, particularly as HDAC inhibitors may induce apoptosis in glucocorticoid-resistant leukaemic cells[29]. Finally, these results indicate that comprehensive evaluation of sequence alterations and epigenetic modifications in relapsed ALL is likely to yield further biological insights and potential therapeutic approaches for this disease.

METHODS SUMMARY

Sequencing of 300 genes was performed by polymerase chain reaction (PCR) and capillary resequencing of whole genome amplified DNA extracted from leukaemic cells obtained at diagnosis and relapse from 23 B-cell progenitor ALL cases. *CREBBP* and *EP300* mutation recurrence testing was performed in an additional 48 diagnosis–relapse B-cell and T-cell ALL samples, and *CREBBP* was also sequenced in 270 ALL and AML samples that did not relapse. All putative mutations were validated as somatic by sequencing of corresponding remission DNA samples, and by sequencing of unamplified tumour and matched normal DNA. All cases had DNA copy number alteration data from Affymetrix 500K or SNP 6.0 microarrays.

***In vitro* functional assays of CREBBP mutants.** H3K18 acetylation, gene expression and cell proliferation were assayed in $Crebbp^{\Delta flox/\Delta flox}$;$Ep300^{\Delta flox/\Delta flox}$ dKO MEFs[23–25] transduced with retroviral supernatants expressing wild-type and mutant *Crebbp* alleles. Dexamethasone and vorinostat drug response assays and all methods are described in full in the online-only Methods.

Full Methods and any associated references are available in the online version of the paper at www.nature.com/nature.

Received 29 June; accepted 1 December 2010.

1. Mullighan, C. G. *et al.* Genome-wide analysis of genetic alterations in acute lymphoblastic leukaemia. *Nature* **446,** 758–764 (2007).
2. Kuiper, R. P. *et al.* High-resolution genomic profiling of childhood ALL reveals novel recurrent genetic lesions affecting pathways involved in lymphocyte differentiation and cell cycle progression. *Leukemia* **21,** 1258–1266 (2007).
3. Mullighan, C. G. *et al.* Genomic analysis of the clonal origins of relapsed acute lymphoblastic leukemia. *Science* **322,** 1377–1380 (2008).
4. Goodman, R. H. & Smolik, S. CBP/p300 in cell growth, transformation, and development. *Genes Dev.* **14,** 1553–1577 (2000).
5. Pui, C. H., Robison, L. L. & Look, A. T. Acute lymphoblastic leukaemia. *Lancet* **371,** 1030–1043 (2008).
6. Harrison, C. J. Cytogenetics of paediatric and adolescent acute lymphoblastic leukaemia. *Br. J. Haematol.* **144,** 147–156 (2009).
7. Mullighan, C. G. *et al.* Deletion of *IKZF1* and prognosis in Acute Lymphoblastic Leukemia. *N. Engl. J. Med.* **360,** 470–480 (2009).
8. Kuiper, R. P. *et al. IKZF1* deletions predict relapse in uniformly treated pediatric precursor B-ALL. *Leukemia* **24,** 1258–1264 (2010).
9. Yang, J. J. *et al.* Genome-wide copy number profiling reveals molecular evolution from diagnosis to relapse in childhood acute lymphoblastic leukemia. *Blood* **112,** 4178–4183 (2008).
10. Vo, N. & Goodman, R. H. CREB-binding protein and p300 in transcriptional regulation. *J. Biol. Chem.* **276,** 13505–13508 (2001).
11. Blobel, G. A. CREB-binding protein and p300: molecular integrators of hematopoietic transcription. *Blood* **95,** 745–755 (2000).
12. Yang, X. J. The diverse superfamily of lysine acetyltransferases and their roles in leukemia and other diseases. *Nucleic Acids Res.* **32,** 959–976 (2004).
13. Schorry, E. K. *et al.* Genotype-phenotype correlations in Rubinstein-Taybi syndrome. *Am. J. Med. Genet. A.* **146A,** 2512–2519 (2008).
14. Miller, R. W. & Rubinstein, J. H. Tumors in Rubinstein-Taybi syndrome. *Am. J. Med. Genet.* **56,** 112–115 (1995).
15. Kung, A. L. *et al.* Gene dose-dependent control of hematopoiesis and hematologic tumor suppression by CBP. *Genes Dev.* **14,** 272–277 (2000).
16. Iyer, N. G., Ozdag, H. & Caldas, C. p300/CBP and cancer. *Oncogene* **23,** 4225–4231 (2004).
17. Kishimoto, M. *et al.* Mutations and deletions of the CBP gene in human lung cancer. *Clin. Cancer Res.* **11,** 512–519 (2005).
18. Shigeno, K. *et al.* Disease-related potential of mutations in transcriptional cofactors CREB-binding protein and p300 in leukemias. *Cancer Lett.* **213,** 11–20 (2004).
19. Radtke, I. *et al.* Genomic analysis reveals few genetic alterations in pediatric acute myeloid leukemia. *Proc. Natl Acad. Sci. USA* **106,** 12944–12949 (2009).
20. Mullighan, C. G. *et al. BCR-ABL1* lymphoblastic leukaemia is characterized by the deletion of Ikaros. *Nature* **453,** 110–114 (2008).
21. Mullighan, C. G. *et al.* Rearrangement of CRLF2 in B-progenitor- and Down syndrome-associated acute lymphoblastic leukemia. *Nature Genet.* **41,** 1243–1246 (2009).
22. Liu, X. *et al.* The structural basis of protein acetylation by the p300/CBP transcriptional coactivator. *Nature* **451,** 846–850 (2008).
23. Kang-Decker, N. *et al.* Loss of CBP causes T cell lymphomagenesis in synergy with p27Kip1 insufficiency. *Cancer Cell* **5,** 177–189 (2004).

24. Kasper, L. H. *et al.* Conditional knockout mice reveal distinct functions for the global transcriptional coactivators CBP and p300 in T-cell development. *Mol. Cell. Biol.* **26,** 789–809 (2006).
25. Kasper, L. H. *et al.* CBP/p300 double null cells reveal effect of coactivator level and diversity on CREB transactivation. *EMBO J.* **29,** 3660–3672 (2010).
26. Dordelmann, M. *et al.* Prednisone response is the strongest predictor of treatment outcome in infant acute lymphoblastic leukemia. *Blood* **94,** 1209–1217 (1999).
27. Pasqualucci, L. *et al.* Inactivating mutations of acetyltransferase genes in B-cell lymphoma. *Nature* doi:10.1038/nature09730 (this issue).
28. Bolden, J. E., Peart, M. J. & Johnstone, R. W. Anticancer activities of histone deacetylase inhibitors. *Nature Rev. Drug Discov.* **5,** 769–784 (2006).
29. Tsapis, M. *et al.* HDAC inhibitors induce apoptosis in glucocorticoid-resistant acute lymphatic leukemia cells despite a switch from the extrinsic to the intrinsic death pathway. *Int. J. Biochem. Cell Biol.* **39,** 1500–1509 (2007).
30. Bordoli, L. *et al.* Functional analysis of the p300 acetyltransferase domain: the PHD finger of p300 but not of CBP is dispensable for enzymatic activity. *Nucleic Acids Res.* **29,** 4462–4471 (2001).

Supplementary Information is linked to the online version of the paper at www.nature.com/nature.

Acknowledgements We thank T. Jeevan, S. Orwick and A. Gibson for technical assistance, B. Schulman for assistance with structural modelling, and B. Woolf and J. Hartigan of Beckman Coulter Genomics for assistance with sequencing. We thank the Tissue Resources Facility of St Jude Children's Research Hospital for providing samples, and the following St Jude core facilities: Vector Development and Production, Flow Cytometry and Cell Sorting, Cell and Tissue Imaging, the Animal Resource Center, and the DNA sequencing and Macromolecular Synthesis laboratories of the Hartwell Center for Bioinformatics and Biotechnology. This study was supported by ALSAC of St Jude and Cancer Center support grant P30 CA021765, and grant number DE018183 (P.K.B.). C.G.M. is a Pew Scholar in the Biomedical Sciences.

Author Contributions C.G.M., P.K.B. and J.R.D. designed the study. S.L.H., L.H., C.G.M., L.A.P. and D.P.-T. performed PCR and sequencing. J.Z. and K.H.B. analysed sequence data. L.H.K. and S.L. performed *in vitro* assays of the functional activity of Crebbp mutants. J.M. analysed genomic data. S.L.H. and J.R.C.-U. performed cell line assays. S.D.B. designed and performed leukaemia cell line drug responsiveness assays. C.-H.P. provided samples and clinical data. C.G.M. wrote the manuscript. All authors reviewed the manuscript.

Author Information Reprints and permissions information is available at www.nature.com/reprints. The authors declare no competing financial interests. Readers are welcome to comment on the online version of this article at www.nature.com/nature. Correspondence and requests for materials should be addressed to C.G.M. (charles.mullighan@stjude.org).

METHODS

Patients and samples. Seventy-one children with matched diagnosis and remission ALL samples were studied, including 61 cases previously studied by SNP microarray analysis[3]. All samples had at least 80% blasts by immunophenotypic and/or morphologic analysis, or were flow-sorted to at least 90% purity before DNA extraction. Sequencing of 300 genes was performed for 23 B-cell progenitor ALL cases. *CREBBP* and *EP300* mutation recurrence testing was performed in an additional 48 diagnosis–relapse B-cell and T-cell ALL samples. Samples obtained at diagnosis from 270 children with AML and ALL who did not experience relapse were also sequenced for *CREBBP* variants. This cohort comprised AML cases with translocation (8;21) *[RUNX1-RUNX1T1]* ($N = 9$), inversion/translocation (16;16) *[CBFB-SMMHC]* ($N = 16$), translocation (15;17) or related rearrangements involving *RARA* ($N = 7$), M7 morphology ($N = 9$), rearrangement of *MLL* ($N = 15$), normal or miscellaneous karyotype ($N = 44$); B-cell progenitor ALL cases with high hyperdiploidy ($N = 13$), *ETV6-RUNX1* ($N = 13$), *TCF3-PBX1* ($N = 13$), rearrangement of *MLL* ($N = 12$), *BCR-ABL1* ($N = 15$), hypodiploidy with 44–45 chromosomes ($N = 10$), normal, pseudodiploid or miscellaneous karyotype ($N = 12$), and T-cell lineage ALL ($N = 82$). The study was approved by the St Jude Children's Research Hospital Institutional Review Board.

CREBBP was also sequenced in 58 AML and ALL cell lines. Cell lines were obtained from the Deutsche Sammlung von Mikroorganismen und Zellkulturen, the American Type Culture Collection, from local institutional repositories, or were gifts from O. Heidenreich (SKNO-1) and D. Campana (OP1). Cells were cultured in accordance with previously published recommendations[31]. The paediatric *BCR-ABL1* B-cell precursor ALL cell line OP1 (ref. 32) was cultured in RPMI-1640 containing 100 units per mililitre penicillin, 100 $\mu g\,ml^{-1}$ streptomycin, 2 mM glutamine and 10% fetal bovine serum. DNA was extracted from 5×10^6 cells obtained during log phase growth after washing in PBS using the QIAamp DNA blood mini kit (Qiagen).

The ALL cell lines were as follows: 380 (*MYC-IGH* and *BCL2-IGH* B-cell precursor), 697 (*TCF3-PBX1*), ALL-SIL (T-cell ALL with *HOX11-TCRD* and *NUP214-ABL1*), AT1 (*ETV6-RUNX1*), B1 (*MLL-AF4*), BV173 (chronic myelogenous leukaemia in lymphoid blast crisis), CCRF-CEM (T-cell ALL with *TAL-SIL*), CTV-1 (T-cell ALL with *TAL1-TRB*), DND41 (T-cell ALL with *HOX11L2/TLX3-BCL11B* alteration), HPB-ALL (T-cell ALL with *HOX11L2/TLX3-BCL11B*), HSB-2 (T-cell ALL), Jurkat (T-cell ALL), Kasumi-2 (*TCF3-PBX1*), KARPAS 45 (T-cell ALL with *MLL-MLLT7*), KE-37 (*MYC-TRAD*), KOPT-K1 (T-cell ALL with *LMO2/TTG2-TRD*), LOUCY (T-cell ALL), MHH-CALL-2 (hyperdiploid B-cell precursor ALL), MHH-CALL-3 (*TCF3-PBX1*), MHH-CALL-4 (*IGH@-CRLF2*), MOLT3 (T-cell ALL), MOLT 13 (T-cell ALL), MOLT 15 (T-cell ALL; may be identical to CTV-1), MKB-1 (T-cell ALL line; may be subline of CCRF-CEM), MOLT4 (T-cell ALL), MUTZ5 (IGH@-CRLF2), NALM-6 (B-cell precursor ALL), OP1 (*BCR-ABL1*), P12/Ichikawa (T-cell ALL), PEER (T-cell ALL with *NKX2-5-BCL11B* and *NUP214-ABL1*), PF-382 (T-cell ALL), Reh (*ETV6-RUNX1*), REX (T-cell ALL), RPMI 8402 (T-cell ALL with *LMO1/TTG1-TRAD, SIL-TAL1/SCL*), RS4;11 (*MLL-AF4*), SD1 (*BCR-ABL1*), SKW3 (T-cell ALL, may represent KE-37), SUP-B15 (*BCR-ABL1*), SUP-T1 (T-cell ALL with *TRB-NOTCH1*), SUP-T11 (T-cell ALL with *TRA/D-TCL1*), TALL-1 (T-cell ALL), TOM-1 (*BCR-ABL1*), U-937 (*PICALM-AF10*), UOCB1 (*TCF3-HLF*) and YT (natural killer cell leukaemia).

The AML cell lines were as follows: CMK (FAB M7), HL-60 (FAB M2), K-562 (chronic myelogenous leukaemia in myeloid blast crisis), Kasumi-1 (*RUNX1-RUNX1T1*), KG-1 (myelocytic leukaemia), ME-1 (*CBFB-MYH11*), ML-2 (*MLL-AF6*), M-07e (FAB M7), Mono Mac 6 (*MLL-AF9*), MV4-11 (*MLL-AF4*), NB4 (*PML-RARA*), NOMO-1 (*MLL-AF9*), PL-21 (FAB M3), SKNO-1 (*RUNX1-RUNX1T1*) and THP-1 (FAB M5).

Genomic sequencing. DNA from diagnosis, relapse and remission samples was amplified by Phi29 polymerase (RepliG, Qiagen). Resequencing of all coding exons was performed by PCR and capillary sequencing. Initial sequencing was performed by Beckman Coulter Genomics (formerly Agencourt Bioscience and Cogenics Danvers). Mutations were validated by sequencing whole genome amplified remission DNA for variants not present in the SNP database, dbSNP[33]. *CREBBP* and *EP300* variants not present in matched germline samples were validated by repeat PCR and sequencing of unamplified DNA. PCR primer sequences, PCR reaction conditions, thermal cycling parameters and sequence traces are available upon request. Expression of CREBBP variants was confirmed by reverse transcription using Superscript III (Life Technologies) and PCR using either Phusion HF DNA polymerase (New England Biolabs) or BD Advantage DNA polymerase (Clontech). To detect low levels of relapse-acquired mutations in diagnosis samples, (RT-)PCR products were cloned into pGEM-T-Easy (Promega) and at least 24 colonies were bidirectionally sequenced.

Sequence analysis. Base calls and quality scores were determined using the program PHRED[34,35]. Sequence variations including substitutions and insertion/deletions (indel) were analysed using the SNPdetector[36] and the IndelDetector[37] software. A usable read was required to have at least one 30-base pair (bp) window in which 90% of the bases have a PHRED quality score of at least 30. Poor-quality reads were filtered before variation detection. The minimum thresholds of secondary-to-primary peak ratio for substitution and indel detection were set to be 20% and 10%, respectively. All sequence variations were annotated using a previously developed variation annotation pipeline[38]. Any variation that did not match a known polymorphism (defined as a dbSNP record that does not belong to the OMIM SNP nor COSMIC somatic variation database[33,39]) and resulted in a non-silent amino acid change was considered a putative mutation. Sequence variants were visualized using Consed[40].

Western blotting. Western blotting of CREBBP/Crebbp of either whole-cell lysates or nuclear extracts[41] of leukaemia cell lines and MEFs was performed using anti-HA and anti-CREBBP (A22, Santa Cruz Biotechnology) antibodies.

Structural modelling of CREBBP and EP300 HAT domain mutations. The HAT domain amino acid sequences of CREBBP and EP300 are highly homologous. The mutations in the HAT domain in EP300, and the homologous EP300 mutations corresponding to the CREBBP HAT mutations, were visualized using the solved crystal structure of a semi-synthetic heterodimeric EP300 HAT domain in complex with a bi-substrate inhibitor, Lys-CoA[22] (http://dx.doi.org/10.2210/pdb3biy/pdb)[42]. Visualization was performed using Pymol[43].

In vitro analyses of the effects of CREBBP mutations on target gene expression, histone acetylation, and cell proliferation MEF isolation and culture were performed as previously described[25]. MEF treatments used were for 90 min with 10 μM forskolin + 100 μM IBMX or ethanol vehicle, 4 h with 1 μM dexamethasone or ethanol, or 1 h treatment with 100 $\mu g\,ml^{-1}$ Poly I:C or PBS followed by a wash, medium change and incubation for 3 h before harvesting of cells into TRIzol (Life Technologies). Generation of mouse *Crebbp* (CBP)-HA retroviral constructs and retroviral transduction were performed as previously described[25]. Residue position numbering in the CBP–HA constructs is based on the conserved residue in human CREBBP. For all retroviral experiments except proliferation assays, retroviral transductions were 70% or higher. Quantitative RT–PCR, western blot and immunofluorescence protocols were described previously[25]. H3K18Ac (ab1191) (Abcam), HA-11 monoclonal antibody against the HA epitope (Boehringer Mannheim), CREBBP (A-22) and EP300 (N-20) (Santa Cruz Biotechnology) were used for immunofluorescence. CBP/p300 antiserum (2574) used for immunofluorescence was generated against GST-p300 1-328, but detects both CBP and p300 similarly by immunofluorescence. For proliferation assays, $Crebbp^{flox/flox}$;$Ep300^{flox/flox}$;*YFP* MEFs were infected with CBP retrovirus, then endogenous *CBP* and *p300* were deleted with adenovirus-Cre after 2 days (day 1 being the day following overnight adenovirus-Cre treatment). Yellow fluorescent protein (YFP) expression was activated in deleted cells. Proliferation assays were commenced with one million YFP^+ MEFs on day 1 and were passaged every 2–3 days. The total number of YFP^+ cells on day 11 was calculated from the total cell number and from YFP^+ percentage as determined by flow cytometry.

Gene expression profiling of MEFs. Total RNA was extracted from untransduced dKO MEFs and dKO MEFs transduced with wild-type and mutant Crebbp alleles treated with vehicle or 1 μM dexamethasone for 4 h. RNA was processed and hybridized to HT MG-430 PM gene expression arrays (Affymetrix) according to the manufacturer's instructions. Probe sets were selected for visualization and validation that meet the criteria of threefold induction by dexamethasone in all four dKO + Crebbp-HA + dexamethasone samples and which had a minimal level of expression that is above twice the background (≥3.1) for the same four samples.

Dexamethasone and vorinostat drug response assays. The activities of dexamethasone (APP Pharmaceuticals) and vorinostat (Selleck Chemicals) were evaluated against nine T-cell ALL cell lines (Jurkat, HPB-ALL, SUPT1, MKB1, REX, P12/Ichikawa, TALL-1, LOUCY and PEER) using an MTT ((3-(4,5-dimethylthiazol-2-yl)-2,5-diphenyltetrazolium bromide) cell viability assay. Cells were treated with the indicated drug concentration for 72 h. Data were analysed as the mean percentage of dimethyl sulphoxide (DMSO)-treated control cells at each concentration. IC_{50} values were calculated from the dose–response curves using nonlinear regression analysis as implemented in the computer software program Prism version 5.0 (GraphPad Software). For each drug and cell line, three to four independent experiments were performed with six replicates at each concentration.

31. Drexler, H. G. *The Leukemia-Lymphoma Cell Line Facts Book* 1st edn (Academic Press, 2001).
32. Manabe, A. *et al.* Interleukin-4 induces programmed cell death (apoptosis) in cases of high-risk acute lymphoblastic leukemia. *Blood* **83,** 1731–1737 (1994).
33. Sherry, S. T. *et al.* dbSNP: the NCBI database of genetic variation. *Nucleic Acids Res.* **29,** 308–311 (2001).

34. Ewing, B., Hillier, L., Wendl, M. C. & Green, P. Base-calling of automated sequencer traces using phred. I. Accuracy assessment. *Genome Res.* **8,** 175–185 (1998).
35. Ewing, B. & Green, P. Base-calling of automated sequencer traces using phred. II. Error probabilities. *Genome Res.* **8,** 186–194 (1998).
36. Zhang, J. *et al.* SNPdetector: a software tool for sensitive and accurate SNP detection. *PLOS Comput. Biol.* **1,** e53 (2005).
37. Zhang, J. *et al.* Systematic analysis of genetic alterations in tumors using Cancer Genome WorkBench (CGWB). *Genome Res.* **17,** 1111–1117 (2007).
38. Zhang, J., Rowe, W. L., Struewing, J. P. & Buetow, K. H. HapScope: a software system for automated and visual analysis of functionally annotated haplotypes. *Nucleic Acids Res.* **30,** 5213–5221 (2002).
39. Bamford, S. *et al.* The COSMIC (Catalogue of Somatic Mutations in Cancer) database and website. *Br. J. Cancer* **91,** 355–358 (2004).
40. Gordon, D., Albajian, C. & Green, P. Consed: a graphical tool for sequence finishing. *Genome Res.* **8,** 195–202 (1998).
41. Andrews, N. C. & Faller, D. V. A rapid micropreparation technique for extraction of DNA-binding proteins from limiting numbers of mammalian cells. *Nucleic Acids Res.* **19,** 2499 (1991).
42. Berman, H., Henrick, K. & Nakamura, H. Announcing the worldwide Protein Data Bank. *Nature Struct. Biol.* **10,** 980 (2003).
43. DeLano, W. L. The PyMOL Molecular Graphics System. ⟨http://www.pymol.org⟩ (2002).